

# PROCEEDINGS OF SPIE

[SPIDigitalLibrary.org/conference-proceedings-of-spie](https://SPIDigitalLibrary.org/conference-proceedings-of-spie)

## Tomosynthesis method for depth resolution of beta emitters

Thomy Mertzaniidou, Nick Calvert, David Tuch, Danail Stoyanov, Simon Arridge

Thomy Mertzaniidou, Nick Calvert, David Tuch, Danail Stoyanov, Simon Arridge, "Tomosynthesis method for depth resolution of beta emitters," Proc. SPIE 10953, Medical Imaging 2019: Biomedical Applications in Molecular, Structural, and Functional Imaging, 109531G (15 March 2019); doi: 10.1117/12.2511753

**SPIE.**

Event: SPIE Medical Imaging, 2019, San Diego, California, United States

# Tomosynthesis method for depth resolution of beta emitters

Thomy Mertzani<sup>a</sup>, Nick Calvert<sup>b</sup>, David Tuch<sup>c</sup>, Danail Stoyanov<sup>a</sup>, and Simon Arridge<sup>a</sup>

<sup>a</sup>Centre for Medical Image Computing, University College London, UK

<sup>b</sup>Department of Medical Physics and Biomedical Engineering, University College London, UK

<sup>c</sup>Lightpoint Medical, London, UK

## ABSTRACT

The motivation of this study derives from the need for tumour margin estimation after surgical excision. Conventional beta autoradiography of beta emitters can be used to image tissue sections providing high spatial resolution compared to in-vivo molecular imaging. However, it requires sectioning of the specimen and it provides a 2D image of the tissue. Imaging of the 3D tissue sample can be achieved either by imaging sequential 2D sections, which is time-consuming and laborious, or by using a specialised detector for imaging that records the particles' direction, in addition to their position, when they hit the detector. In this work we investigate whether a novel beta-tomosynthesis approach can be used for depth resolution of beta emitters. The technique involves acquiring multiple 2D images of the intact tissue sample while the detector rotates around the sample. The images are then combined and used to reconstruct the 3D position of the sources from a limited angle of conventional 2D autoradiography images. We present the results from Geant4 forward simulations and the reconstructed images from a breast tissue sample containing a Fluorine-18 positron emission source. The experiments show that the proposed method can provide depth resolution under certain conditions, indicating that there is potential for its use as a 3D molecular imaging technique of surgical samples in the future.

**Keywords:** molecular imaging, autoradiography, tomosynthesis, Monte Carlo methods

## 1. INTRODUCTION

Breast cancer is the most common type of cancer in women worldwide. In the UK alone 55,000 cases of invasive breast cancer were diagnosed in 2014. However, with advances in early detection and management the survival rates are generally good. An increasing number of women diagnosed can now avoid radical mastectomy and undergo a breast conserving surgery instead, where only the cancerous tissue is removed sparing the remaining healthy breast tissue, having the same long-term survival rates.<sup>1</sup> Ensuring that there are no positive margins on the excised specimen is crucial to confirm that all cancerous tissue has been removed and eliminate the need for another surgery.

The use of molecular imaging, such as Positron Emission Tomography (PET), has enabled the visualisation of in-vivo cellular function within the body, by imaging the gamma rays resulting from the annihilation of positrons that are emitted from an injected radiopharmaceutical, typically Fluorine-18.<sup>2</sup> Despite the advantages of PET, imaging the annihilation gammas provides limited spatial resolution,<sup>3</sup> typically 1 – 2 mm. On the contrary, beta autoradiography<sup>4</sup> can be used to image directly the positrons emitted from the same tracers, providing high spatial resolution for ex-vivo imaging of excised samples, after the administration of the radioactive isotope in-vivo. This can find application in oncology, for example for tumour margin estimation after surgery or imaging of the surgical cavity in-vivo with an endoscope,<sup>5,6</sup> as the mean path length of positrons within the tissue is in the order of 2 mm.

Typically both beta endoscopes and beta autoradiography provide a 2D image of the tissue (the surface directly attached to the endoscope or a thin tissue slice respectively). For ex-vivo imaging, 3D spatial information of the source can be enabled by imaging sequential 2D sections<sup>7</sup> which is destructive for the tissue, time-consuming, laborious and prone to image-registration errors. This has mainly found application in small animal studies.<sup>8</sup> More recently 3D spatial localisation of the source has been proposed by imaging the tissue using a

---

Further author information: Send correspondence to T.M. E-mail: t.mertzani@cs.ucl.ac.uk

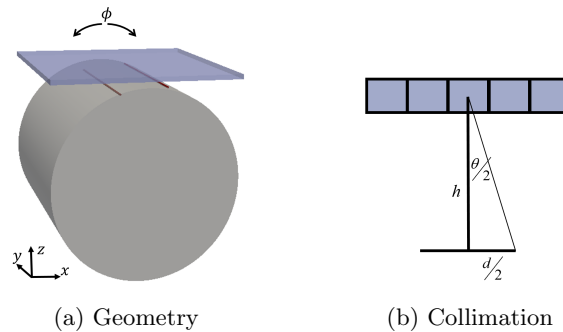


Figure 1: Illustration of (a) the geometry and (b) the collimation angle used in the modelling. In (a) the breast tissue appears grey, the detector blue and the beta emitting sources in red. In (b) each square corresponds to a grid position of the detector.

specially-adapted detector which records the particles' direction in addition to their position when they reach the detector.<sup>9,10</sup>

The acquisition of multiple 2D projection images over a complete  $180^\circ$  angle around the imaging body has revolutionised medical imaging. However this complete angle range is not possible for all applications. Limited angle tomography allows some depth resolution of the anatomy by acquiring projection images over a limited angular range and then reconstructing a 3D image using a number of reconstruction techniques, such as unfiltered and filtered back-projection, iterative methods etc.<sup>11</sup> The last decades this approach has been applied successfully in clinics for in-vivo breast cancer imaging, using a technique named X-ray tomosynthesis.<sup>12,13</sup>

Inspired by the X-ray limited angle tomography methods that overcome the limitation of a single 2D projection image, we investigate the potential of a novel beta imaging technique, namely beta-tomosynthesis, where multiple 2D beta autoradiographs are acquired with either the detector rotating around the sample or vice-versa, similarly to the concept of X-ray tomosynthesis. The 3D position of the source in the sample is then reconstructed from the 2D images. The advantage of this approach is that it provides 3D information without requiring sectioning of the sample, which is destructive, or the use of special equipment, such as a specially-adapted detector, which is not widely available. We demonstrate the potential of this technique using forward beta autoradiography simulations for a breast tissue sample with a Fluorine-18 source, which is widely used clinically. The 3D position is then reconstructed using unfiltered backprojection.

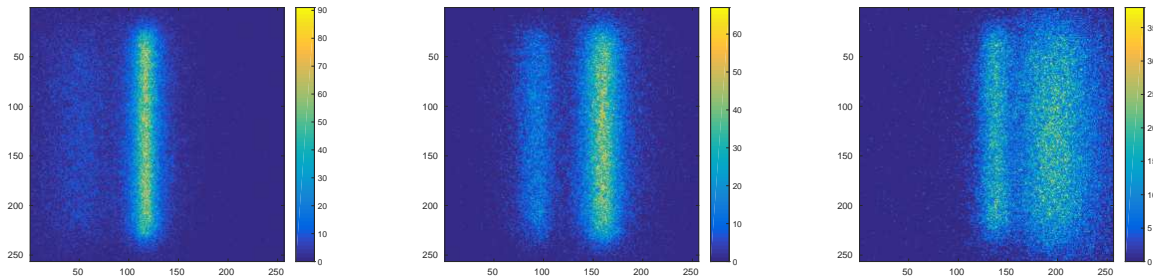
## 2. METHODOLOGY

This study investigates whether beta-tomosynthesis can be used for depth resolution of beta emitters in a two-step approach. First, for the forward modelling Monte Carlo (MC) simulations are performed in Geant4 to generate a number of 2D beta autoradiographs acquired at a different angle. These are then used by the reconstruction method to determine the 3D position of the sources in the tissue from the 2D images.

### 2.1 Forward modelling

MC simulations were performed using the Geant4 toolbox,<sup>14</sup> which models the passage of particles through matter. In our experiments we have modelled a cylindrical block of glandular tissue that represents a breast surgery specimen. Two  $^{18}\text{F}$  sources were inserted at different depths from the surface to simulate the uptake of the  $^{18}\text{F}$  - *FDG* tracer in two tumour locations. A Calcium Fluoride ( $\text{CaF}_2$ ) crystal scintillator that converts the positrons to optical light was placed as an ideal detector above the tissue to record the number of photons, their location and their wavelength. The geometry is shown in Figure 1a. The dimensions of the tissue sample are: length  $l_t = 10$  mm and radius  $r_t = 5$  mm, the sources are also cylindrical (length  $l_s = 8$  mm and radius  $r_s = 5$   $\mu\text{m}$ ) and they were placed at  $0$   $\mu\text{m}$  and  $300$   $\mu\text{m}$  depth from the surface of the tissue.

For the simulation of the positron-emitting  $^{18}\text{F}$  sources, positrons were generated at a random position within the source, with a random momentum direction and a random energy sampled from the  $^{18}\text{F}$  spectrum. The world around the tissue and the detector was modelled as air.



(a)  $\phi = -20^\circ$

(b)  $\phi = 0^\circ$

(c)  $\phi = 20^\circ$

Figure 2: 2D autoradiographs acquired at different angles  $\phi$ . The bar on the right is placed at the surface of the cylindrical tissue (and therefore the number of detected photons is higher), while the bar on the left is at 300  $\mu\text{m}$  depth.

To enable reconstruction from multiple 2D images, the direction of the particles needs to be known or limited to a small angle range. To enable the latter, we have introduced collimation in the simulations by accepting the photons that arrive from a limited angle at each grid location of the detector, as shown in Figure 1b. In our experiments we have used a collimator with height  $h = 250 \mu\text{m}$  and hole diameter  $d = 31.25 \mu\text{m}$ , corresponding to an acceptance angle of  $\theta = 7.1^\circ$ . Therefore the detector was placed at a distance  $h$  from the tissue sample. The choice of these collimation parameters was empirical and it was a trade-off between ensuring a small enough acceptance angle to restrict the direction of the incoming particles, while allowing enough particles to traverse and be detected to get a signal. For the simulations we assume that the septal wall thickness is zero.

To acquire the 2D autoradiographs we have rotated the tissue sample around the central axis of the cylinder (Y), which is equivalent to rotating the detector around the sample. There were 61 radiographs simulated in total for a range of  $\phi = [-60, 60]^\circ$  with a  $2^\circ$  step (Figure 1a).

For each radiograph acquisition there were 100,000 events simulated. The output of each simulation is the sum of all the detected photons computed at a discretised grid of  $256 \times 256$  for a  $10 \times 10 \text{ mm}$  detector. The wavelength of each photon is also recorded using 1 nm wide bins.

## 2.2 Reconstruction

For the reconstruction we have used an unfiltered backprojection algorithm, which is commonly used in tomography applications.<sup>15</sup> It is computed using the ‘iradon’ function in Matlab, with no filter and linear interpolation in pixel space.

## 3. RESULTS

Some examples of the simulated 2D radiographs for a  $256 \times 256$  detector and 100,000 events are illustrated in Figure 2. Following unfiltered backprojection, examples of the reconstructed planes within the tissue are shown in Figure 3.

The difference between the reconstructed planes in Figures 3a,3b and the ones in their vicinity can be difficult and subjective to judge visually. Therefore, and to obtain some quantitative measure, for each one of the transverse (XY) reconstructed planes close to the position of the sources we have taken the line profile at the centre of the Y dimension and have fitted a two-term Gaussian model:

$$f(X) = \frac{A_1}{\sigma_1 \sqrt{2\pi}} e^{-\frac{1}{2} \left( \frac{x-\mu_1}{\sigma_1} \right)^2} + \frac{A_2}{\sigma_2 \sqrt{2\pi}} e^{-\frac{1}{2} \left( \frac{x-\mu_2}{\sigma_2} \right)^2}. \quad (1)$$

At the plane that corresponds to the position of each source the corresponding Gaussian should have the lowest standard deviation  $\sigma$  and also a high peak. The line profiles and the Gaussians fitted for planes 4 and 11 in Figures 3a,3b are shown in Figure 4a. We can now see that one of the two Gaussians (blue) is narrower at the

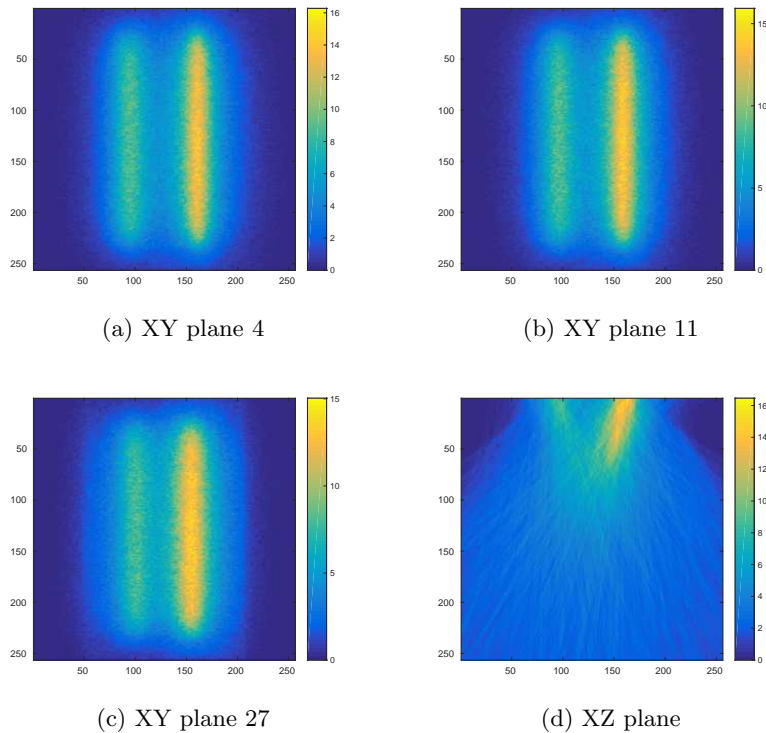


Figure 3: Example planes of the reconstructed volume for: a) The transverse XY plane at grid position  $Z = 4$ , where the source at the surface (on the right) should be in focus, b) The transverse XY plane at grid position  $Z = 11$ , where the source at  $300 \mu\text{m}$  (on the left) should be in focus, c) The transverse XY plane at grid position  $Z = 27$ , deeper within the tissue, where neither of the sources are in focus (notice the image is more blurry) and d) The XZ plane in the centre of the  $Y$  dimension of the reconstructed volume.

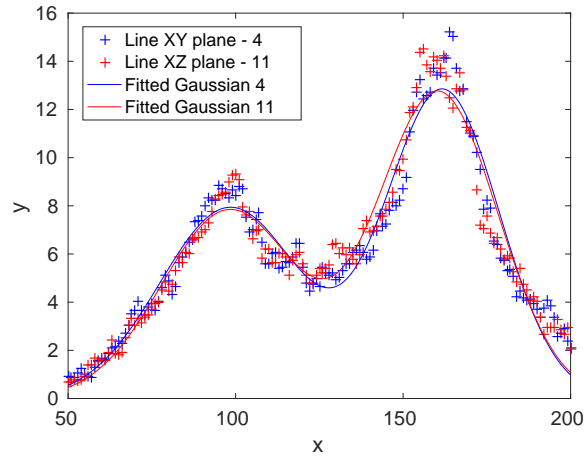
peak on the right (corresponding to the source on the surface), while the other one (red) is narrower at the peak on the left (corresponding to the other source, at  $300 \mu\text{m}$  depth). Table 1 shows the standard deviations of the fitted Gaussians for all the planes at the vicinity.

We can see that the lowest values are for planes 5 and 12, which are adjacent to the ones expected (4 and 11). The difference between planes 4–5 and 11–12 is negligible as illustrated in Figure 4b. Therefore we can conclude that following this technique we can identify the depth at which each source is positioned following some quantitative analysis. As it can be seen in Figure 2 this information cannot be extracted from one of the 2D autoradiographs alone.

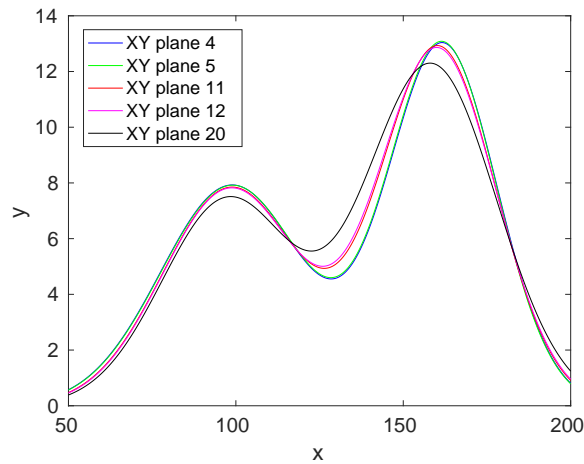
If we continue looking at the standard deviations of the Gaussians at larger depths ( $Z > 12$ ) we can see that they do get smaller, however their peak is also progressively lower as illustrated with the black curve in Figure 4b and indeed the Area Under the Curve (AUC) is also decreasing, therefore providing a confirmation that the source is not positioned at a greater depth.

#### 4. DISCUSSION

This study is the first work, to the best of our knowledge, that investigates whether a beta-tomosynthesis technique can be used for depth resolution of beta-emitting sources. For this purpose the forward simulations were performed using the software package Geant4 and the reconstruction followed using a simple unfiltered backprojection algorithm. The results indicate that depth resolution is possible following some quantitative analysis of the reconstruction results, while depth discrimination within the reconstructed volume is difficult to assess with simple visual inspection.



(a) The line profiles and fitted two-term Gaussians for different transverse (XY) reconstruction planes in the volume (4 and 11).



(b) The fitted Gaussians for XY planes 4, 5, 11, 12 and 20.

Figure 4: The line profiles and fitted two-term Gaussians for different transverse reconstruction planes in the volume. In both figures the x axis corresponds to the grid position in X (the total grid size is 256) and the y axis corresponds to the intensity of the detector (ie. the number of photons detected).

Table 1: The standard deviations ( $\sigma_1$  and  $\sigma_2$ ) corresponding to the two-term Gaussians fitted to the line profiles of different XY planes  $Z$  of the reconstructed volume. The lowest values are highlighted in bold, corresponding to planes  $Z = 5$  and  $Z = 12$ .

	$Z = 3$	$Z = 4$	$Z = 5$	$Z = 7$	$Z = 9$	$Z = 10$	$Z = 11$	$Z = 12$
$\sigma_1$	16.20	16.19	<b>16.17</b>	16.33	16.67	16.92	17.17	17.45
$\sigma_2$	21.34	21.31	21.31	21.14	20.86	20.65	20.53	<b>20.38</b>

The results are encouraging, however this study is the first step towards investigating the potential of beta-tomosynthesis, as the 2D radiographs have been generated with MC simulations assuming an ideal geometry of a cylindrical tissue sample and an ideal detector, without taking into account any noise other than the statistical noise resulting from the MC simulations. Future work also includes taking into account the septal thickness of the collimation. Further studies are required to repeat similar experiments in the lab using initially phantom and then small animal ex-vivo data and capture the images of the scintillator with a Charge-Coupled Device camera. An analysis will also need to be performed to determine the acquisition time requirements in a clinical setting. These will be the next step before applying this approach to human surgical specimen and potentially in the future to intra-operative imaging of surgical cavities. It is worth noting that for clear margins in breast conserving surgery and prostatectomy samples tumour should not be present at the surface and within 1 or 2 mm depth in the tissue. Given the path length of positrons, beta-tomosynthesis can be an appropriate technique for depth discrimination within this range.

## 5. CONCLUSION

We have presented a method to perform beta-tomosynthesis with a scope to determine the depth of radioactive sources within the tissue, without destroying the sample or requiring any specially-adapted detector. The results demonstrate the use of this approach on simulated data for a breast tissue sample with two  $^{18}F$  sources, a widely available radioisotope in oncology, positioned at different depths. This technique has a future potential for use in oncology, both for margin estimation after excision in the operating theatre, and in the future for imaging the surgical cavity with a hand-held probe (in breast surgery) or an endoscope (in prostate surgery). Further work includes validation using phantom and animal data.

## ACKNOWLEDGMENTS

This work was supported by the Engineering and Physical Sciences Research Council grant EDCLIRS (EP/N022750/1).

## REFERENCES

- [1] Veronesi, U., Cascinelli, N., Mariani, L., Greco, M., Saccozzi, R., Luini, A., Aguilar, M., and Marubini, E., "Twenty-year follow-up of a randomized study comparing breast-conserving surgery with radical mastectomy for early breast cancer," *New England Journal of Medicine* **347**(16), 1227–1232 (2002).
- [2] Gambhir, S. S., "Molecular imaging of cancer with positron emission tomography," *Nature Reviews Cancer* **2**(9) (2002).
- [3] Levin, C. S. and Hoffman, E. J., "Calculation of positron range and its effect on the fundamental limit of positron emission tomography system spatial resolution," *Physics in medicine and biology* **44**(3), 781 (1999).
- [4] Stumpf, W. E., [*Drug localization in tissues and cells*], IDDC-Press, Chapel Hill, NC (2003).
- [5] Daghighian, F., Mazziotta, J. C., Hoffman, E. J., Shenderov, P., Eshaghian, B., Siegel, S., and Phelps, M. E., "Intraoperative beta probe: a device for detecting tissue labeled with positron or electron emitting isotopes during surgery," *Medical physics* **21**(1), 153–157 (1994).
- [6] Piert, M., Carey, J., and Clinthorne, N., "Probe-guided localization of cancer deposits using [ $^{18}F$ ] fluorodeoxyglucose," *The Quarterly Journal of Nuclear Medicine and Molecular Imaging* **52**(1), 37 (2008).
- [7] Solon, E. G., Schweitzer, A., Stoeckli, M., and Prideaux, B., "Autoradiography, maldi-ms, and sims-ms imaging in pharmaceutical discovery and development," *The AAPS journal* **12**(1), 11–26 (2010).
- [8] Solon, E. G. and Kraus, L., "Quantitative whole-body autoradiography in the pharmaceutical industry: Survey results on study design, methods, and regulatory compliance," *Journal of pharmacological and toxicological methods* **46**(2), 73–81 (2001).
- [9] Ding, Y., Caucci, L., and Barrett, H. H., "Directional charged-particle detector with a two-layer ultrathin phosphor foil," in [*Nuclear Science Symposium and Medical Imaging Conference (NSS/MIC), 2014 IEEE*], 1–4, IEEE (2014).
- [10] Ding, Y., Caucci, L., and Barrett, H. H., "Charged-particle emission tomography," *Medical Physics* **44**(6), 2478–2489 (2017).

- [11] Friel, J., "Sparse regularization in limited angle tomography," *Applied and Computational Harmonic Analysis* **34**(1), 117–141 (2013).
- [12] Dobbins III, J. T. and Godfrey, D. J., "Digital x-ray tomosynthesis: current state of the art and clinical potential," *Physics in medicine and biology* **48**(19), R65 (2003).
- [13] Tingberg, A., "X-ray tomosynthesis: a review of its use for breast and chest imaging," *Radiation protection dosimetry* **139**(1-3), 100–107 (2010).
- [14] Allison, J., Amako, K., Apostolakis, J., Araujo, H., Dubois, P. A., Asai, M., Barrand, G., Capra, R., Chauvie, S., Chytrcek, R., et al., "Geant4 developments and applications," *IEEE Transactions on Nuclear Science* **53**(1), 270–278 (2006).
- [15] Kak, A. C. and Slaney, M., [*Principles of computerized tomographic imaging*], SIAM (2001).